

---

## Towards standard test artefacts for synchronous tracking of human-exoskeleton knee kinematics

---

### Roger Bostelman

Smart HLPR, LLC,  
NIST,  
Frederick, MD, USA  
Email: roger.bostelman@nist.gov

### Ann Virts and Soocheol Yoon

Intelligent Systems Division,  
NIST,  
Gaithersburg, MD, USA  
Email: ann.virts@nist.gov  
Email: soocheol.yoon@nist.gov

### Mili Shah

Department of Mathematics,  
The Cooper Union,  
New York, NY, USA  
Email: mili.shah@cooper.edu

### Ya-Shian Li-Baboud\*

Software Systems Division,  
NIST,  
Gaithersburg, MD, USA  
Email: ya-shian.li-baboud@nist.gov  
\*Corresponding author

**Abstract:** A repeatable evaluation of human-exoskeleton kinematics is needed to assess an exoskeleton's impact on worker biomechanics and safety. Standard measurement methods and metrics facilitate technology adoption and effective specification of the exoskeleton's intended use. This study assesses the feasibility and repeatability of a measurement method that enables synchronous tracking of human and exoskeleton kinematics using a set of lower-limb human motion capture test artefacts and exoskeleton motion capture plates. Experimental validation was conducted on 30 subjects. The inter-trial repeatability of the human knee joint angle was within 1.2° to 2.7° and within 1.3° to 3.1° for the exoskeleton joint angle (50th to 99th percentile). To apply the measurement of the test artefacts rigid body position and orientation, two potential metrics, human-exoskeleton fit and stability, were implemented based on the exoskeleton-human alignment offset and the stability of the exoskeleton frame.

**Keywords:** motion capture repeatability; exoskeleton test methods; human motion; capture test artefacts; human-exoskeleton interaction; standard measurement artefacts; synchronous human-exoskeleton tracking; knee kinematics; human-exoskeleton fit; human-exoskeleton stability; human-exoskeleton alignment.

**Reference** to this paper should be made as follows: Bostelman, R., Virts, A., Yoon, S., Shah, M. and Li-Baboud, Y-S. (2022) 'Towards standard test artefacts for synchronous tracking of human-exoskeleton knee kinematics', *Int. J. Human Factors Modelling and Simulation*, Vol. 7, Nos. 3/4, pp.171–203.

**Biographical notes:** Roger Bostelman is a research associate in the Intelligent Systems Division at the National Institute of Standards and Technology after retiring from NIST with 41 years of service. He chairs the ASTM F48.03 on exoskeleton test methods and environments standards subcommittees. Roger has designed, built, and tested mechanical systems and their interface electronics on autonomous vehicles, robot cranes, and robot arms. He holds a PhD in Computer Science from the University of Burgundy, France. He has written over 120 publications, and he holds seven patents.

Ann Virts is the Project Leader of the Mobility Performance of Robotic Systems and is also the Associate Project Leader for the Emergency Response Robots project in the Fire Risk Reduction in Communities program. She developed test methods, artefacts, and datasets that measure the performance and safety characteristics of mobile and wearable robots within manufacturing/industrial environments. She interfaces with emergency responders and robot technology developers, and meets complex technical and logistical demands of demanding response robot field exercises. Her past contributions include leading data collection efforts and participating in field exercises for several DARPA and Army Research Laboratory projects.

Soocheol Yoon is a research associate in the Intelligent Systems Division at NIST. His current work focuses on performance measurement systems for industrial autonomous vehicle and exoskeleton under ASTM F45 and F48 standard development technical committee. His research interests include markerless pose estimation methods and integration of camera sensors for measurement of human-exoskeleton interactions towards the development of standard test methods. He received his PhD in Industrial Engineering at Pohang University of Science and Technology (POSTECH) in South Korea.

Mili Shah is an Associate Professor of Mathematics at The Cooper Union for the Advancement of Science and Art and a research associate at NIST. She received her PhD from the Computational and Applied Mathematics Department at Rice University. Her research interests involve applying numerical linear algebra to real life problems. In the past, this included areas such as molecular dynamics and facial recognition. She is working with NIST on markerless pose estimation to measure human-exoskeleton interactions, camera calibration, and registration problems which have applications in computer vision, manufacturing, and robotics.

Ya-Shian Li-Baboud is a computer scientist in the Software Systems Division at NIST. She performs sensor integration and analysis to track human-exoskeleton kinematics. She researches methods to synchronise data sources for distributed measurements in the smart grid, mobile robot, and quantum research network testbeds. She supports standards development for IEEE and ASTM. Her research interests include distributed measurement and analysis algorithms. She received her MS in Computer Science from George Washington University.

---

## 1 Introduction

Accelerating the production and the adoption of exoskeletons for a wide range of industrial, emergency response, health, and other applications require objective performance standards for safety evaluation and effective application. The estimated exoskeleton market value was at \$241 million in 2020 and expected to reach \$3.387 billion by 2026 (*Exoskeleton Market Size 2020*). While qualitative and quantitative methods exist to measure exoskeleton impact on human muscle activity, discomfort, and task performance, there are limited standards-based and repeatable measurement methods to specify and assess the intended use, safety, and performance of exoskeletons. Research and development of standard measurement and test methods for exoskeletons remain an ongoing effort (Lowe et al., 2019) and is needed to support the safety and performance evaluation of industrial exoskeletons.

### 1.1 Background

Exoskeletons are being developed for a broad range of industries including manufacturing, shipping, construction, healthcare, emergency response, to support the worker during tasks with heavy, prolonged, and repetitive loads to reduce musculoskeletal strains on the body such as the knee, back, and shoulders. Lower limb exoskeletons are intended to support the worker with repetitive or prolonged kneeling and squatting tasks (Pillai et al., 2020). Like the human-machine interface, the human-exoskeleton interface is the place at which the independent systems meet and act on or communicate with each other. Human-exoskeleton system interactions and performance are dependent on the person, the intended tasks, the exoskeleton's mechanisms, and constraints. As the industry continues to develop standard performance test methods for exoskeletons, some of the fundamental design criteria include safety and ergonomic support to prevent musculoskeletal injuries.

In manufacturing metrology, standard methods for system performance evaluation include a series of direct measurements of the system components and through the measurement of manufactured test artefacts (Moylean et al., 2014). Like manufacturing test artefacts, the test artefacts in this study are defined as a test component intended for standardisation and designed to support the quantitative evaluation of human-exoskeleton kinematics. Standard test artefacts provide a basis for comparison for different human-exoskeleton systems performing a specified task. Standard test artefacts can also be used to:

- 1 demonstrate improvements in human-exoskeleton systems
- 2 verify human-exoskeleton performance
- 3 understand human-exoskeleton interactions and limitations.

Prior studies have indicated that marker clusters on the shank may be comparable and, at times, slightly more repeatable than the placement of skeletal marker sets at anatomical landmarks with rotational errors about the longitudinal axis on the order of  $\pm 4^\circ$  (Collins et al., 2009; Manal et al., 2000). Shank, thigh, and knee markers on anatomical landmarks can lead to translation errors on the order of 10 mm to 40 mm due to soft tissue movement and up to  $8^\circ$  in rotational error (Peters et al., 2010). Comparison of the Helen Hayes marker set relative to a set of thigh and shank marker clusters showed the sagittal

knee joint angle estimates derived from the two methods had correlation in the range of 0.814 to 0.935, with slightly higher repeatability for the marker cluster (Collins et al., 2009). Having a rigid measurement structure has the potential to be more amenable to standardisation, rather than a skeletal model that has dependencies on the marker placement of the test administrator, the test subject anthropometry, the task, and the exoskeleton. Marker placement can be time consuming and difficult to position correctly, reliably, and securely across different trials, test administrators, and test subjects. The motion capture test artefacts were motivated by the need to reduce exoskeleton occlusion of the skeletal marker set and to simplify marker sets for synchronously tracking the position and orientation of the tibia and femur segments of the exoskeleton and its user. To demonstrate how the measurements can be applied, the kinematics information computed from the human motion capture test artefacts were used to derive two metrics:

- 1 exoskeleton fit-to-user
- 2 human-exoskeleton system stability.

Fit, as measured by the human-exoskeleton alignment, and the stability of the human-exoskeleton, are two basic safety performance factors, and therefore prioritised in the study of measurement methods for exoskeleton performance.

## *1.2 Review of measurement methods for human and exoskeleton kinematics*

In order to assess an exoskeleton's fit-to-user, one measurement method is the use of a motion capture system. Optical motion tracking is one of the clinically validated methods used to assess human kinematics and biomechanics. Optical tracking systems (OTS) have been validated for their uncertainty and repeatability by many studies to measure both large-scale and small-scale measurements in static and dynamic contexts. In static tests for small-scale measurements, the precision and repeatability for within-trial and between-trial standard deviations were less than 30  $\mu\text{m}$ , while the accuracy was less than 1.56% of the total displacement for out-of-plane motion (Schmidt et al., 2009). For measuring dynamic human motion, the challenges in using pre-defined skeletal marker models include marker position errors caused by soft tissue movement (Peters et al., 2010), repeatability of marker placement, and the assumptions of common anthropometric models across the human population. In landmark marker placement based on models such as Helen Hayes (Kadaba et al., 1990), a marker displacement error of 1 cm at the hip can lead to a 2° joint angle estimation error. Errors caused by markers directly placed on soft tissue have been reported to cause differences of 6° to 24.3° in knee joint angle estimation for a flexion task (Brown and Stanhope, 1995; Akbarshahi et al., 2010). Another clinical validation methodology of marker sets in comparison to bone segment data from magnetic resonance imaging resulted in a maximum difference of 22 mm in translation and 15° in rotation (Sangeux et al., 2006). Furthermore, while it is known that marker placement is susceptible to test administrator variability, the degree of kinematic measurement sensitivity to marker placement variability remains a subject for further research (McFadden et al., 2020). For capturing the interaction between the human and the exoskeleton kinematics, there is the additional challenge that the landmark models may be occluded by the exoskeleton itself, and therefore require modifications (Talaty et al., 2013).

In estimating knee joint angles with marker clusters (Collins et al., 2009; Charlton et al., 2004), the motion capture system tracks the rigid body's position and orientation. In an OTS, a rigid body is defined by a set of at least 3 asymmetrically positioned markers specified by the user. Ideally, the distance between the markers forming the rigid body remain constant. Achieving joint angle measurement accuracy rests on the assumption that marker placement is consistent between trials and between test administrators. For biomechanical tracking of anatomical joints, there also exists a position offset between the relevant anatomical landmark and the rigid body that requires calibration (Cappozzo et al., 2005). Human motion capture test artefacts can be placed relative to externally protruding bone structures that serve as landmarks, such as the ankle bone or the wrist bone. Combining careful placement of motion capture markers and motion capture test artefacts and execution can increase the repeatability of the joint angle estimation. For marker clusters with anatomical calibrations and joint centre estimations, the inter-trial repeatability of joint angle estimation (within a session) ranges from  $1.84^{\circ}$  to  $2.90^{\circ}$  on average (Charlton et al., 2004). Between a cluster-based method and an anatomical landmark marker placement, the relative mean difference of the computed joint angles at various phases of knee flexion and extension ranged from  $-5.8^{\circ}$  [standard deviation (S.D.)  $2.92^{\circ}$ ] to  $2.5^{\circ}$  (S.D.  $3.02^{\circ}$ ) (Collins et al., 2009). Prior studies used knee joint kinetics when assessing human-exoskeleton alignment (Wang et al., 2018), a modified skeletal marker model for joint kinematics to manage exoskeleton occlusions (Mooney and Herr, 2016), a separate kinematic and kinetic analysis between normal and exoskeleton gait models (Barbareschi et al., 2015), an exoskeleton marker model to estimate both human and exoskeleton kinematics (Alvarez et al., 2017), or an exoskeleton model simulation (Tang et al., 2019; Sposito et al., 2020). In addition, studies on human-exoskeleton knee misalignment relied on intentional elongation or shortening of the exoskeleton femur and tibia segments rather than tracking the alignment throughout a task after a test subject has been fitted by a trained test administrator (Zanotto et al., 2015).

Other methods of motion capture, using inertial measurement units (IMUs) can estimate the joint angle of the knee in dynamic motion with an uncertainty between  $1^{\circ}$  and  $11^{\circ}$  (Vlasic et al., 2007; Poitras et al., 2019). While the measurements may have higher uncertainty, IMUs enable more flexible test protocols without the need to be confined to a motion capture volume. Furthermore, with proper alignment and calibration, IMU-based measurement accuracy in the sagittal plane have recently been shown to have a root mean square error (RMSE) below  $3.6^{\circ}$  based on validation with a motion capture system, and with a reproducibility of  $1.1^{\circ}$  (Lebleu et al., 2020). The IMU-based measurement accuracy is often compared with the 'gold-standard' OTS. One limitation is that OTS errors, such as marker ambiguity or occlusion, can confound the IMU error characterisation as both are susceptible to muscle and skin motion when sensors or markers are placed on the limbs. Garment-based motion capture uses colour coded patterns, requiring the test subject to wear specific attire. Using specialised garments, the knee joint angle estimation has been shown to have a measurement repeatability of  $1.16^{\circ}$  up to  $3^{\circ}$  (Biasi et al., 2015).

One of the key benefits of vision-based measurement systems is the ability to minimise the constraints on the test subject of having to move within a spatially limited sensing platform, such as force plates, or to wear additional sensors, such as IMUs. However, there are concerns regarding quantification of human and human-exoskeleton interactions due to measurement, inter-subject, and inter-step variations (Brown and

Stanhope, 1995; Zhang and Collins, 2017). OTS are subject to several instrumentation, implementation, and tracking uncertainties including the motion capture camera placement, motion capture camera resolution, volume size and location, marker placement, skin movement, marker occlusions, activity, individual variability as well as analysis errors such as the validity of mathematical model assumptions (Dorociak and Cuddeford, 1995; Peters et al., 2010).

### *1.3 Exoskeleton performance parameters*

Consistent evaluation methods for the exoskeleton community of manufacturers and users foster clear communication of needs and expectations along with continuous improvement of fit and use protocols to promote safety, comfort, and efficiency of using exoskeletons. Human-exoskeleton misalignment can create additional inertial forces that require more user effort and strain. A key area of innovation in rigid, flexible, and soft exoskeleton and exosuits is the ability to maintain human-exoskeleton alignment, while meeting musculoskeletal support requirements for a set of intended tasks (Wang et al., 2018). It can be a challenge to align lower-limb exoskeletons due to the rotation and translation in 6 degrees of freedom (6DoF) of the human knee joint (Choi et al., 2016; Masouros et al., 2010).

### *1.4 Study objectives*

While marker sets and marker clusters are well-established for human motion tracking, there is limited literature on the measurement methods for synchronous tracking of human-exoskeleton kinematics. The study was intended to address the gaps in the standardisation of measurement methods to assess human-exoskeleton motion in executing industrial tasks. Standard motion capture test artefacts can potentially support exoskeleton manufacturers and users to apply a consistent measurement tool in the development of standard measurement methods. Human-exoskeleton motion capture test artefacts are intended to be applied to industrial exoskeleton performance standards. Industrial exoskeletons include passive exoskeletons providing mechanical support to the test subject. The performance standards include test methods established through working group consensus in evaluating the safety and effectiveness of the exoskeleton in supporting or augmenting the test subject's task execution. Tasks may include load positioning, load alignment, and peg-in-hole, which simulates warehouse loading tasks such as storing and stocking shelves with boxes, aligning heavy or bulky objects such as tires to vehicles, and overhead drilling.

A repeatable measurement methodology is needed to track exoskeleton fit-to-user by evaluating the alignment dynamics, quantify the misalignment, and locate the point of exoskeleton misalignment relative to the subject. Motion capture test artefacts allow characterisation of misalignment in the human-exoskeleton knee joints by synchronously tracking the human-exoskeleton kinematics. Additionally, the three-dimensional (3D) position and orientation of the femur and tibia segments of the test subject and the exoskeleton can potentially be used to evaluate the human-exoskeleton system stability. Identifying the phases where the misalignment errors or instabilities are most significant can help manufacturers and users understand how to better align exoskeleton motion to the user and therefore improve future design, safety, and performance.

The study of the human motion capture test artefacts and the exoskeleton motion capture plates is intended to

- 1 independently and simultaneously track the human and exoskeleton lower-extremity kinematics
- 2 simplify and expedite the test procedure
- 3 allow the subject to wear typical casual attire (e.g., jeans, shirt, and shoes)
- 4 address skeletal marker set occlusions due to the exoskeleton
- 5 determine whether the motion capture test artefacts could track the human and exoskeleton knee kinematics with sufficient repeatability, within  $3^\circ$ , which is comparable to existing marker cluster and skeletal marker sets.

In the context of this study, repeatability is defined as the measurement precision based on the test method described to determine whether the motion capture test artefacts and test plates provide comparable joint angle estimates. A prior study was conducted to assess the fidelity of knee joint angle measurements derived from marker plates relative to the knee joint angle of a simulated skeletal frame (Bostelman et al., 2020). To further expand on the applicability of the motion capture test artefacts and plates in human-exoskeleton motion tracking this study evaluated the repeatability of the derived test subject and exoskeleton knee joint angle measurements

- a within a single subject
- b between 30 subjects.

To further demonstrate the use of synchronous human-exoskeleton knee joint angle estimates, the study implemented two metrics, *exoskeleton fit-to-user* and *human-exoskeleton stability*.

## 2 Experimental method

### 2.1 Test subjects

Thirty self-declared healthy, physically fit test subjects with no injuries at the time of the study gave written consent to participate in the study over a period of four months from July 2018 to November 2018. All test subjects were categorised as typical office or laboratory workers. The test subjects included 10 females and 20 males ranging in height from 155 cm to 183 cm and weighed less than 114 kg to be within the exoskeleton size constraints. Each test subject wore the same passive industrial exoskeleton, providing shoulder, leg, and back support. The exoskeleton included adjustments for arm length, shoulder depth, shoulder support adjustment, shoulder width, torso length, hip width, hip depth, femur segment length, tibia segment length, strap adjustments at the knee, a button to enable lift assistance, a torque switch at the knee, and a lock mode to provide chair-like support. For this study, the *leg assistance* and *knee torque* were enabled, while the shoulder and chair support were disabled. The *leg assistance* provided support to the test

subject during the flexion and extension phases of the knee bend. For all participants, the torque switch at the knee joint was set to high, to provide maximum lift assistance. The leg component of the exoskeleton is about 6.2 kg and is designed to support industrial tasks requiring repeated or prolonged squatting. For consistency, the same test administrator fitted the exoskeleton and the femur and tibia components of the motion capture test artefacts onto all of the test subjects throughout the study.

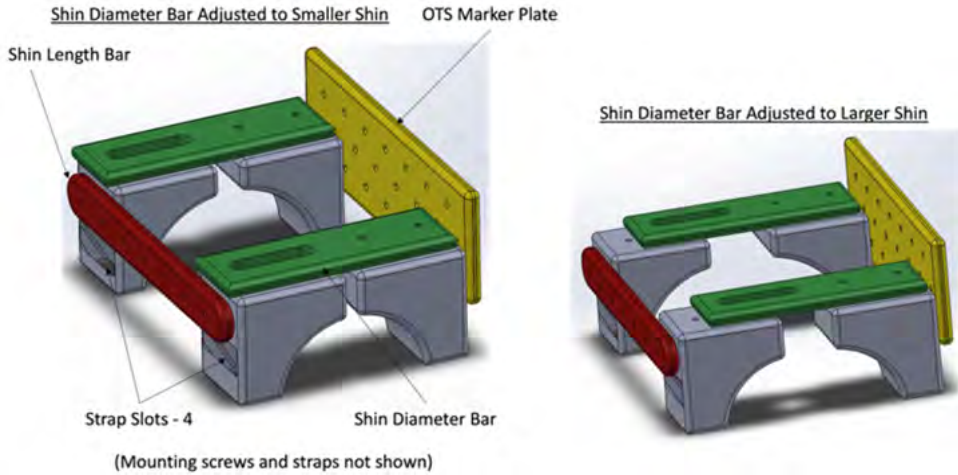
## 2.2 *Motion capture test artefacts*

To simplify the synchronous motion tracking of the test subject and exoskeleton lower extremity position and orientation, a pair of human motion capture test artefacts and exoskeleton motion capture plates were designed and implemented. The femur and tibia components of the human motion capture test artefacts were designed and shown in Figure 1. The designs were 3D printed and provided an adjustable shin and thigh diameter bar to conform to a range of subject sizes.

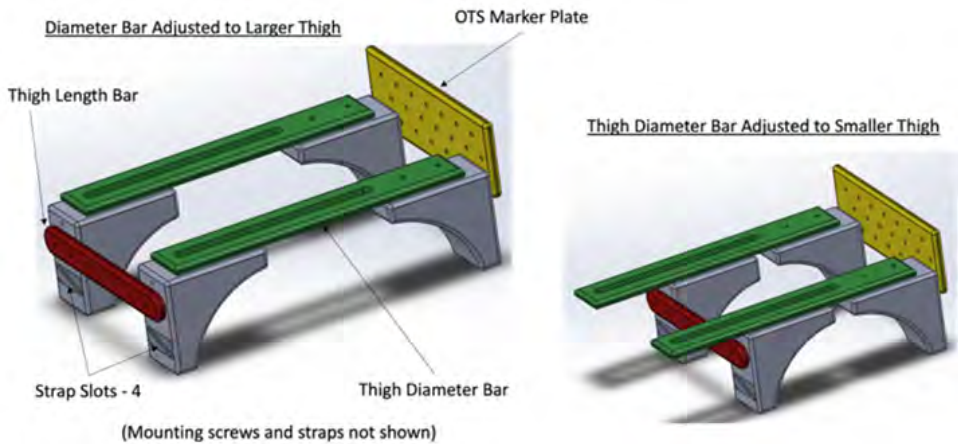
The femur and tibia components of the human motion capture test artefacts were each composed of seven to eight 11 mm passive-reflective markers. Two markers were placed on the front of both the femur and tibia components of the human motion capture test artefacts. On the right side, a 3.81 cm by 15.24 cm 3D printed marker plate was attached with screws. Two exoskeleton motion capture plates (8.89 cm by 15.24 cm) were constructed from 1.5 mm thick aluminum plates mounted to the exoskeleton femur and tibia segments using double-sided adhesives as shown in Figure 2. Four 11 mm diameter, passive-reflective markers were asymmetrically attached to each plate to mitigate marker ambiguity. The purpose of the plate was to provide a plane to align with the exoskeleton motion capture plates.

In a prior study, a 3D printed knee test apparatus, referred to as the test apparatus, was developed to simulate the femur, knee, and tibia bone segments. The simulation provided a means to evaluate the uncertainty and repeatability at which the simulated femur, knee, and tibia segments can be tracked using the two sets of exoskeleton and human motion capture plates (Bostelman et al., 2020). The 3D printed knee provided a model that emulated the linear and rotational motion of the knee. Attached to the 3D printed knee were two aluminum bars to simulate the femur and tibia, providing the skeletal frame. The 3D CAD model isolates motion to the sagittal plane. The prior test evaluated the human and exoskeleton motion capture plates on the test apparatus, as shown in Figure 2. Figure 2(b) and 2(c) shows a CAD model of the 3D printed knee with rotational and translational components. The model uses a centre axis screw that moves along a linear slot [see Figure 3(b)] along with an outer screw that rotates in a circular slot having two tangential curves of different radii to model the human knee. The errors based on the angle estimates from the motion capture plates were determined to be  $0.81^\circ \pm 0.35^\circ$  for the exoskeleton motion capture plates and  $1.17^\circ \pm 0.55^\circ$  for the human motion capture plates, in static trials shown in Figure 3. The standard deviation of the joint angle estimates ranged from  $1.1^\circ$  to  $1.3^\circ$ .

**Figure 1** Adjustable 3D printed human motion capture test artefacts to be attached to the lower extremity for tracking the knee joint angle, (a) human motion capture test artefact (tibia component) attached to the shin above the ankle (b) human motion capture test artefact (femur component) attached to the thigh above the knee (c) human motion capture plates attached to test artefacts (see online version for colours)

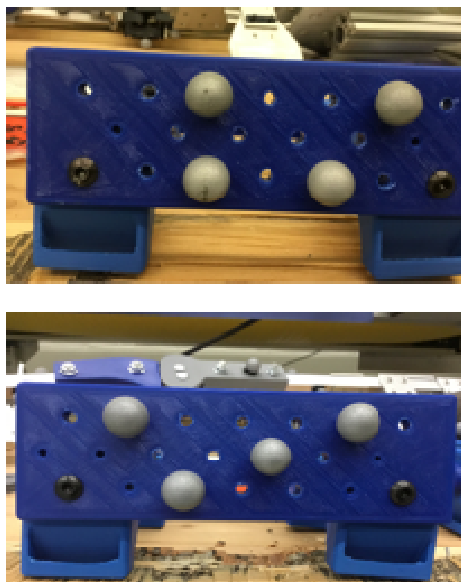


(a)



(b)

**Figure 1** Adjustable 3D printed human motion capture test artefacts to be attached to the lower extremity for tracking the knee joint angle, (a) human motion capture test artefact (tibia component) attached to the shin above the ankle (b) human motion capture test artefact (femur component) attached to the thigh above the knee (c) human motion capture plates attached to test artefacts (continued) (see online version for colours)

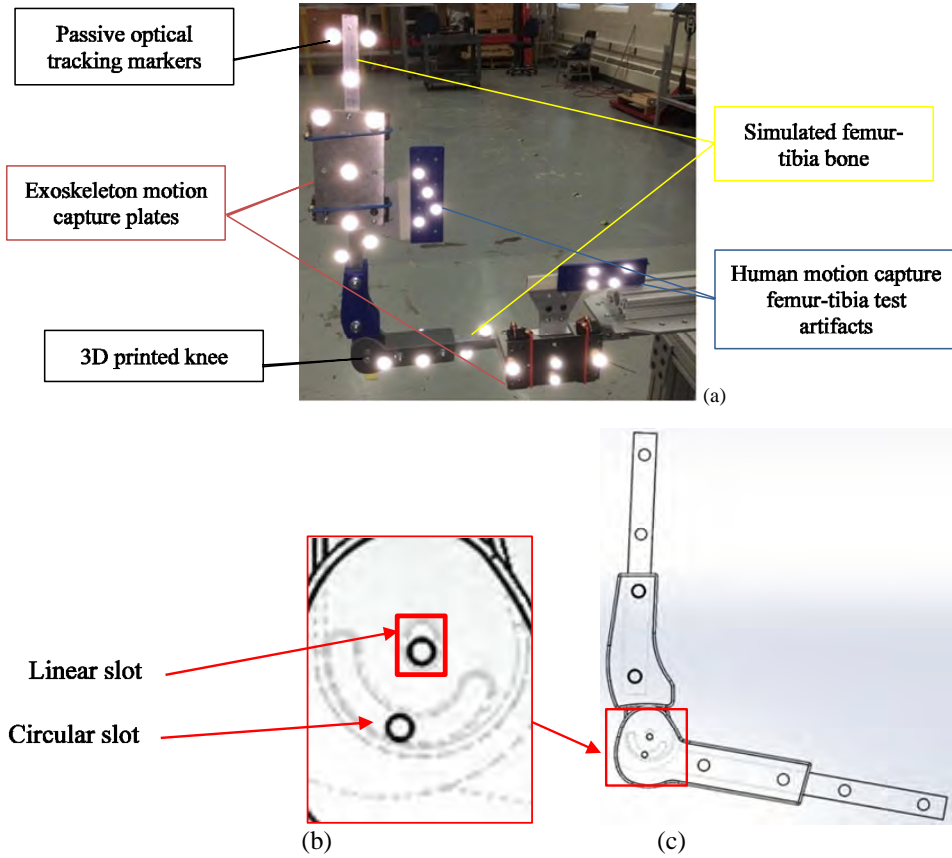


(c)

The human motion capture test artefact design was adjusted during the study to reduce the rotation and slippage. Slippage can be observed in the kinematic trajectories. Changes in the relative position of the human motion capture artefacts can be detected by observing the peak flexion angle of each squat. A negative slope tangent to the maxima of the computed knee joint angles indicated the motion capture artefacts had moved during the test. This occurred in the initial test subjects. To improve upon the design, buckles were integrated into the human motion capture test artefacts to comfortably tighten the straps around the limb (August 2018). As the test method evolved, additional straps were attached to the test subject just above the knee as a visual marker of the knee location and one was attached between the test subject's belt and the femur human motion capture test artefact to further prevent slippage. The tibia component of the human motion capture test artefact was anchored at the ankle, just above the shoe, as shown in Figure 4.

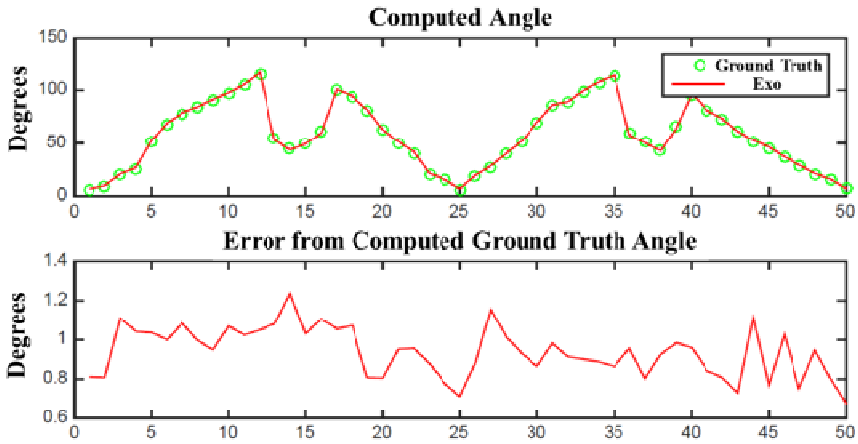
The exoskeleton motion capture plates were intended to provide a plane aligned with the exoskeleton to track the knee flexion-extension angle. By providing both exoskeleton motion capture plates and human motion capture test artefacts, the relative angles between the rigid bodies can be independently assessed. The exoskeleton motion capture plate was attached to the outside of the exoskeleton and followed the exoskeleton kinematics. The attachment surface of the exoskeleton is rigid and flat, and therefore the plate does not affect the use of the exoskeleton.

**Figure 2** Human and exoskeleton motion capture plates with passive-reflective markers were attached to the test apparatus with a 3D printed knee (see online version for colours)



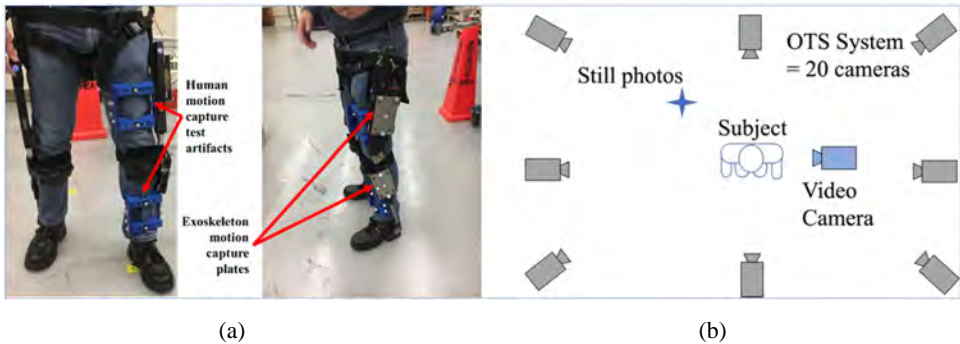
Notes: The test apparatus was used to determine the static and dynamic angle estimation uncertainty between the joint angle determined by the simulated skeletal frame and the joint angle determined by the exoskeleton (metallic) and human (blue) motion capture plates. Below, the CAD model of the 3D printed knee test apparatus, where (b) highlights the printed knee design's rotational and translational components of the knee kinematics; and (c) shows the skeletal frame to which the artefacts can be positioned to understand the joint position and orientation error relative to the motion capture plate marker sets and position

**Figure 3** Comparison of flexion-extension joint angle measurements between exoskeleton motion capture plates and the skeletal frame of the 3D printed knee test apparatus (see online version for colours)



Note: The bottom graph shows the joint angle difference between the angles computed using the passive markers on the skeletal frame and the passive markers on the exoskeleton motion capture plates

**Figure 4** Human motion capture test artefacts and exoskeleton motion capture plates are shown in, (a) the exoskeleton motion capture plates can be adhered to the femur (proximal) and tibia (distal) segments of lower limb exoskeletons (b) the test subject trials were recorded in a motion capture volume with 20 motion capture cameras (figure is not to scale nor are all the OTS cameras included), a video camera, and a still camera



### 2.3 Data acquisition

The tests were performed in a 9 m by 22 m motion capture area. The motion capture cameras were mounted at a height of approximately 2.7 m and 4.3 m off the ground. As shown in Figure 4, the measurement devices included a still camera, a video camera, and 20 Optitrack<sup>1</sup> Prime 41 cameras acquiring data at a rate of 120 frames per second (fps) using Motive version 1.10. The optical motion capture cameras were triggered using the manufacturer provided synchronisation system. The OTS was calibrated per manufacturer's documentation on a weekly basis using a calibration bar (Motive Documentation: Calibration, 2017). The two human motion capture test artefacts and the two exoskeleton motion capture plates enabled the OTS to track the human and exoskeleton femur and tibia segments as rigid bodies. The test subject's left foot was placed in the same location in the capture volume for most subjects. A few test subjects adjusted their rotation about the marked position in the capture volume to maximise the perceived marker visibility, based on the extent of marker jitter from the motion capture software. Issues encountered during the data acquisition included exoskeleton occlusions and damage to the human motion capture test artefact markers. This caused a marker to fall in a few incidents and the marker was removed in subsequent tests. Scraping against the exoskeleton or while walking with the motion capture test artefacts can cause damage to the markers. There were no issues with the exoskeleton motion capture plates interfering with the function of the exoskeleton limb; however, there were times when the test subject's lower arm occluded the exoskeleton motion capture plate. Test subjects were made aware of the possible occlusion, which can interfere with the test subject's task completion method and balance.

### 2.4 Test protocol

Most of the test subjects had an opportunity to become accustomed to the exoskeleton for at least 30 minutes. The acclimation phase allowed the test subject to become accustomed to the human-exoskeleton interface and can reduce imbalance and kinematic variability (McNamara, 2020). Each test subject was fitted with the exoskeleton and most test subjects had performed an industrial task of load positioning. From the load positioning testbed, the test subject walked approximately 100 m to the motion capture testbed. The human motion capture test artefacts were strapped onto the test subject to provide two rigid bodies for capturing the femur and tibia leg segments. The human tibia test artefact was placed directly above the test subject's left foot and the femur component of the human motion capture test artefact was placed directly above the test subject's left knee.

The test subject completed at least five trials. In the first trial, the test subject stood stationary for 10 s. In the second trial, the test subject performed a squat for 10 s. The first two trials were intended to provide a baseline to estimate the test subject's extension and flexion angles. The test subject performed three sets of three squats to measure the human-exoskeleton knee kinematics. The test protocol was developed to provide a quick simulation of a repetitive squatting motion that the exoskeleton was designed to support. A high-resolution video camera was used to record each of the test subject trials at 30 fps.

For safety, the test protocol allowed test subjects to hold on to a chair for balance and support as needed. However, the chair was one of the potential sources of occlusion that can lead to outliers in the marker data. Other sources of marker ambiguity and occlusion included any reflections from the floor, reflections from the exoskeleton motion capture

plates, exoskeleton straps, and other parts of the subject such as the arms. Upon completing the five trials, a visual review of the data was performed by the researchers to verify minimal missing marker data. If significant marker data loss was observed, the test subject repeated one or more trials.

Adjustments were made over time to the test, such as how the human motion capture test artefact was secured to the user. The motion capture adjustments primarily occurred within the first few test subjects. Some of these adjustments improved the data quality over time. Other experimental protocol differences between test subjects included the location and orientation of the test subject in the motion capture testbed and the amount of time the subject worked with the exoskeleton prior to the test trials.

## 2.5 Human-exoskeleton knee joint angle estimation

The human knee joint's motion is constrained to the rotational directions about the three planes: sagittal, coronal, and transverse (Grood and Suntay, 1983). Similar to prior studies with respect to human-exoskeleton knee joint motion tracking, this study focused on the rotation about the sagittal plane (Önen et al., 2013; Knaepen et al., 2014). The knee joint angle was computed from the femur and tibia rigid body quaternions (Cloete and Scheffer, 2008). This provided a simple method to be invariant to subject rotation within the capture volume and to avoid singularity (Diebel, 2006).

The algorithm to assess repeatability was comprised of three steps:

- 1 *OTS data*: For each of the 30 subjects, the first step was to acquire the orientation of the femur,  $f$ , and the tibia,  $t$ , from the subject's dynamic knee bend trials represented as a quaternion,  $q$ , comprised of  $q_x$ ,  $q_y$ ,  $q_z$ , and  $q_w$ , for both the femur and the tibia segments of the human motion capture test artefacts and the exoskeleton motion capture plates. For analysis, the position and orientation of the femur and tibia components of the human motion capture test artefacts can be used to provide a relative estimate of the human knee joint angle. Each human motion capture test artefact component's marker cluster was used to form a rigid body. Each rigid body was then tracked by the OTS during the trials. The tracking software provided raw 3D marker position data as well as the rigid body's position and orientation in 6DoF. The orientation was represented as quaternions.
- 2 *Angle estimation and joint kinematics*: The second step was to compute the exoskeleton and human knee joint angles over time within each trial, interpolate the outliers as needed, plot the knee joint angle kinematics, and derive the mean and standard deviation for each trial. The rotation quaternion,  $q$ , represents the joint angle rotation derived from the quaternion multiplication of the complex conjugate of the proximal segment (femur) and the distal segment (tibia) relative to the knee joint as shown in equation (1).

$$q = f * t \tag{1}$$

The complex conjugate is defined as shown in equation (2).

$$f^* = f_0 - f_1i - f_2j - f_3k \tag{2}$$

The angle (in degrees) between the human and exoskeleton femur and tibia rigid bodies were computed as shown in equation (3).

$$\theta(\mathbf{q}) = 2 * \arctan 2\left(\sqrt{q_x^2 + q_y^2 + q_z^2}, q_w\right) * \frac{180}{\pi} \quad (3)$$

Outliers were detected by replacing any data points that were 3 standard deviations above the maximum flexion (Masouros et al., 2010) with the previous data point. Additional outliers were detected using the median absolute deviation (MAD) with a sliding window of 120 frames (or within 1 s) as defined by (Matlab Documentation: Filloutliers, 2017):

$$MAD = |\theta_i - \text{median}(\theta)| \quad (4)$$

The algorithm then proceeded to estimate the relative angle between the tibial and femoral rigid bodies and to replace outliers by applying a shape-preserving piecewise cubic spline interpolation (Fritsch and Carlson, 1980; Chiari et al., 2005). A piecewise cubic polynomial function was extrapolated over a time interval of 1 s (120 frames) to interpolate any outliers in the computed angle dynamics of the lower-limb exoskeleton. The interpolation was based on the following assumptions:

- a the first derivative of the polynomial is continuous
- b the second derivative is not necessarily continuous to allow for jumps in the data
- c the polynomial preserves monotonicity and convexity of the original data set over the specified time interval.

For the angle derived from the human motion capture test artefacts, no interpolation was needed. The human motion capture test artefacts had a rigid structure with markers surrounding three sides of the leg segment, which likely mitigated effects of marker ambiguity and occlusion and allowed the motion capture software to track the rigid body throughout the task.

The exoskeleton plates had two marker data issues that created outliers for several subjects analysed. First, the exoskeleton straps or the subject's arms may have occluded the exoskeleton femur markers. The second issue was marker ambiguity, potentially due to the reflective surface of the exoskeleton motion capture plates and the floor of the motion capture volume. From the human knee angle trajectory and the interpolated exoskeleton knee angle trajectory, the mean and standard deviation of the recorded angles over time were computed for each trial, for a total of 3 trials per subject.

- 3 *Repeatability*: To assess the intra-subject, inter-trial repeatability of the human motion capture test artefacts and the exoskeleton motion capture plates, the standard deviation of the joint angle for each dynamic trial,  $s_i$  was computed using equation (5), where  $\theta(\mathbf{q}_i)$  is the computed knee joint angle at frame  $i$ ,  $\mu_\theta$  is the mean joint angle for the trial, and  $N$  is the total number of frames from the trial.

$$s_i = \sqrt{\frac{\sum_{i=1}^N |\theta(\mathbf{q}_i) - \mu_\theta|^2}{N-1}} \quad (5)$$

The variability in the standard deviation between the three dynamic trials from the exoskeleton motion capture plates and the human motion capture test artefacts were computed for each subject to determine the intra-subject repeatability,  $s_{it}$ , using

equation (6), with  $M$  and  $s_i$  denoting the number of trials and the computed joint angle standard deviation per trial, respectively.

$$s_u = \sqrt{\frac{\sum_{i=1}^M |s_{t_i} - \mu_{s_i}|^2}{M-1}} \quad (6)$$

The inter-subject repeatability was derived from the empirical cumulative distribution function (CDF) using  $s_u$  from each of the 30 subjects. The repeatability of the human motion capture artefacts and the exoskeleton motion capture plates for a population of human-exoskeleton systems with similar characteristics was inferred from the standard normal CDF based on the experimental data.

## 2.6 Applicable metrics from synchronous human-exoskeleton knee joint angle estimation

Once the intra-subject and inter-subject repeatability of the dynamic joint angle measurements were established, two metrics for evaluating the *exoskeleton fit-to-user* and the *human-exoskeleton stability* were implemented.

### 2.6.1 Exoskeleton fit-to-user

For optimal human-exoskeleton dynamics, the exoskeleton should assist in synchrony with the user. Minimising joint angle difference between the exoskeleton and the test subject's knee would reduce interference to the user's movement. Therefore, the metric used to evaluate the exoskeleton fit to the user was to simply compute the mean angle difference between the angle of the exoskeleton motion capture plates and the angle of the human motion capture test artefacts during the static, maximum flexion trial for each test subject. For each test subject, a fit offset,  $\theta_{fit_i}$ , based on the mean exoskeleton joint angle,  $\mu_{\theta_e}$ , and the mean human joint angle,  $\mu_{\theta_h}$ , of all frames captured, was computed as:

$$\theta_{offset_i} = \left| \mu_{\theta_e} - \mu_{\theta_h} \right| \quad (7)$$

The mean human-exoskeleton alignment offset from the study of  $S$  subjects,  $\mu_{offset}$ , was computed as:

$$\mu_{offset} = \frac{\sum_{i=1}^S \theta_{offset_i}}{S} \quad (8)$$

To account for the measurement bias between the angle derived for the exoskeleton (from the exoskeleton motion capture plates) and angle derived for the human (from the human motion capture artefacts), the mean of the offset from the subject was removed. The estimated alignment between the exoskeleton and the test subject was computed as knee joint angle offset, mean removed:

$$\theta_{fit_i} = \left| \theta_{offset_i} - \mu_{offset} \right| \quad (9)$$

The exoskeleton fit-to-user for a population with similar characteristics was inferred from the standard normal CDF based on the experimental data.

### 2.6.2 Human-exoskeleton stability

A *human-exoskeleton stability* metric was implemented based on the exoskeleton's stability among the test subjects. The metric would indicate from the sample of subjects, the stability of the human-exoskeleton system while performing a specific task. Imagine the test subject is in a fixed location, standing perfectly balanced. The study used an exoskeleton with a mechanical articulation at the knee joint with a single degree of freedom, and therefore if attached properly and securely to the test subject, the plane of the exoskeleton leg should be perpendicular to the ground. The average normal to the exoskeleton plane would also ideally be fixed, except for the measurement noise. Unless the average exoskeleton plane is parallel to the plane derived from the marker positions at a specific instant in time, human-exoskeleton instabilities, other exoskeleton plane deviations due to the interaction between the test subject's and exoskeleton's motion, and measurement noise would cause the angle between the instantaneous normal vector and the average normal vector of the exoskeleton plane to deviate over the flexion and extension phases of the knee joint. For the metric to apply, it was assumed that:

- 1 the exoskeleton has a single degree of freedom about the knee joint
- 2 the test subject remained in a relatively fixed position and orientation
- 3 the exoskeleton leg was securely attached to the test subject.

Therefore, instability in the human-exoskeleton system can be observed as deviations in the angle of the normal vector to the exoskeleton plane.

The algorithm used to compute the balance angle was based on an optimal plane approximation using the 3D position data ( $x, y, z$ ) from the markers on each of the exoskeleton rigid bodies using the Singular Value Decomposition. The instantaneous optimal exoskeleton plane was based on mean-centred marker position data from the exoskeleton proximal (femur) plate,  $F$ , and exoskeleton distal (tibia) plate,  $T$ , for each frame, and computed as  $P_i = [F T]$ . The average optimal plane of the exoskeleton leg was computed as  $P_{avg} = \frac{1}{N} \sum_{i=1}^N P_i$  and normalised as a unit vector,  $E_{Avg} = \frac{E_{Avg}}{\|E_{Avg}\|}$ . The

balance angle tracks the angle between the average normal vectors of the exoskeleton plane,  $E_{Avg}$ , and the instantaneous normal vector,  $E_i$ , computed for each frame. The human-exoskeleton system stability while performing a specific type of task for a population with similar characteristics was inferred from the standard normal CDF based on the experimental data.

## 3 Results

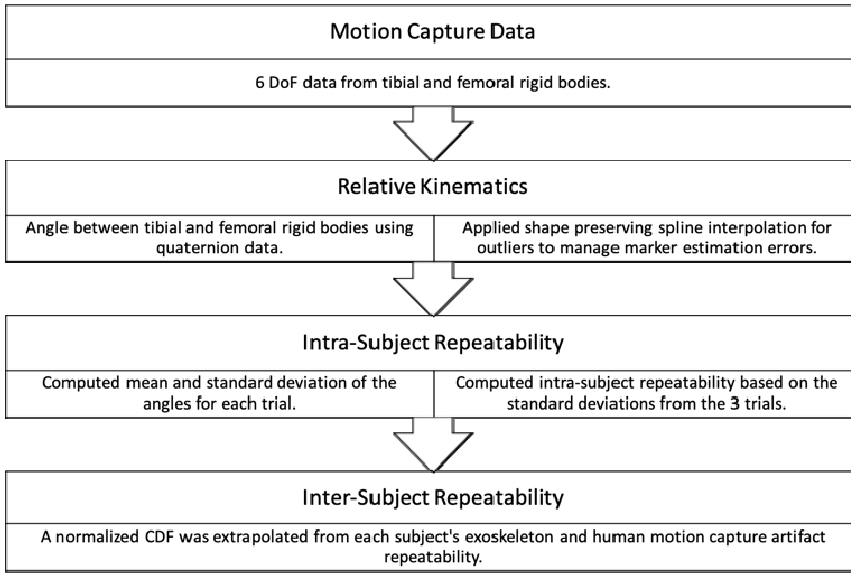
This study evaluated the feasibility of using human motion capture test artefacts and exoskeleton motion capture plates by analysing the *measurement repeatability* of the test subject and exoskeleton knee joint angles. The analysis was conducted with a repeatability criterion within  $3^\circ$ , comparable to existing marker cluster and skeletal

marker sets based on the literature review. Two metrics derived from the joint angle measurements, the *exoskeleton fit to user* and *human-exoskeleton system stability*, were illustrated.

### 3.1 Measurement repeatability

To evaluate the measurement method, the first step was to gauge the repeatability of the human motion capture test artefacts on the test subjects as shown in Figure 5.

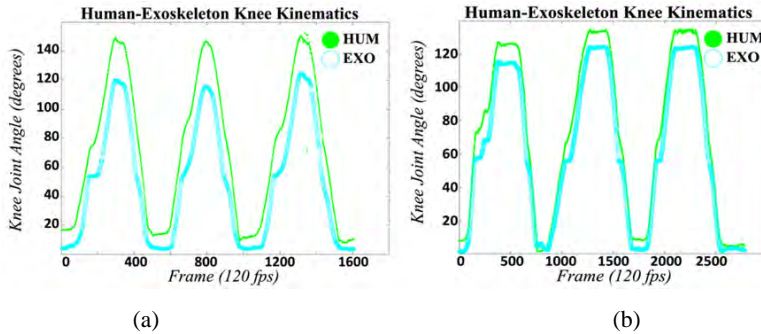
**Figure 5** Motion capture test artefacts’ repeatability analysis process for independent tracking of the exoskeleton knee articulation and the human knee joint



The estimated human and exoskeleton knee joint angles for each data frame are visualised in a time series as shown in Figure 6. Figure 6(a) shows larger angle differences between the estimated exoskeleton and subject’s knee joint angles. The evaluation of the video showed the exoskeleton knee joint was not aligned with the subject’s knee. Figure 6(b), which was evaluated as a ‘good fit’, showed better alignment, but a deviation remains during the maximum flexion phase.

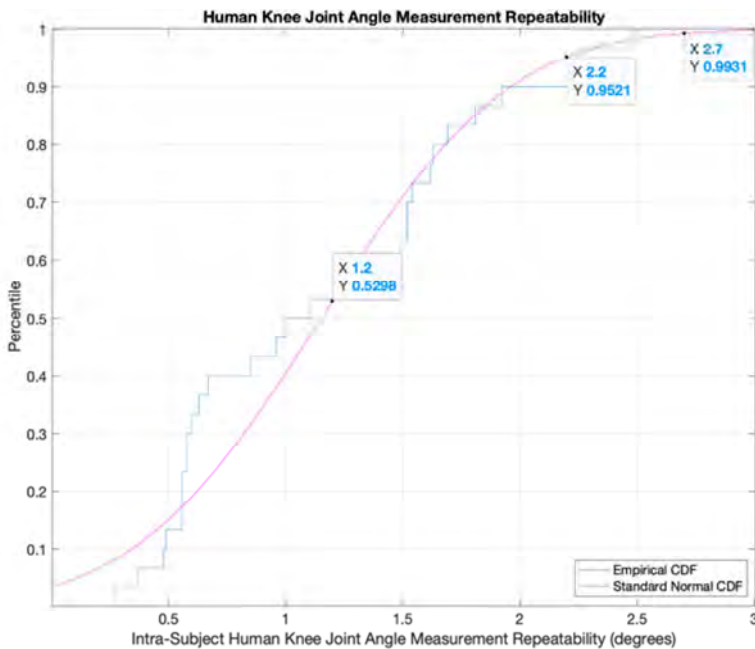
The repeatability of the knee joint angle estimation based on the human motion capture test artefacts was 1.2° at the 50th percentile and around 2.7° at the 99th percentile [see Figure 7(a)]. The repeatability of the exoskeleton articulation angle estimation based on the exoskeleton motion capture plates was 1.3° at the 50th percentile and around 3.1° at the 99th percentile [Figure 7(b)].

**Figure 6** Kinematic trajectory of exoskeleton knee articulation and human knee joint angle where subject performed 3 squats, (a) larger knee joint angle differences between the exoskeleton and the human indicate exoskeleton misalignment during the peak flexion phase (b) some deviation between the exoskeleton and human knee joint angle occurred during the peak flexion phase with a ‘good fit’, which may be due to the alignment of the marker cluster relative to the femur and tibia bones



Note: The exoskeleton kinematic trajectory included outlier interpolation due to marker ambiguity.

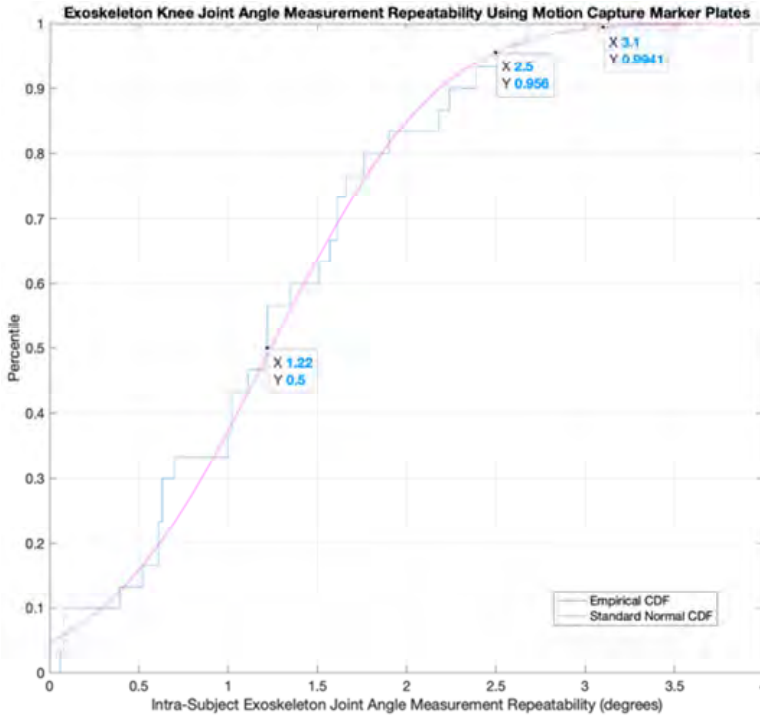
**Figure 7** The inter-subject repeatability was derived from the empirical CDF using  $s_{ii}$  from each of the 30 subjects (see online version for colours)



(a)

Notes: The experimental data was plotted against the standard normal CDF. The human motion capture test artefact and the exoskeleton motion capture plate repeatability of the population were based on the test subject data. Plot (a) and (b) show the human and exoskeleton, respectively, knee joint angle measurement repeatability at the median, 95th, and 99th percentiles.

**Figure 7** The inter-subject repeatability was derived from the empirical CDF using  $s_u$  from each of the 30 subjects (continued) (see online version for colours)



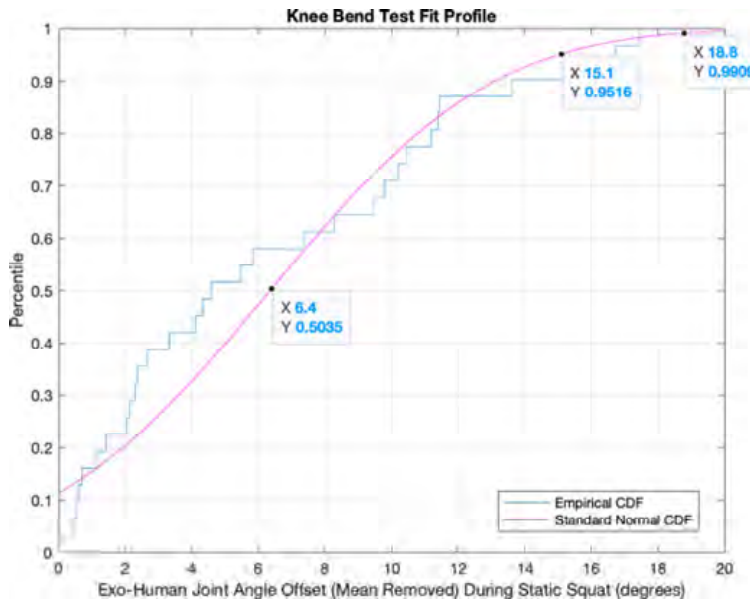
(b)

Notes: The experimental data was plotted against the standard normal CDF. The human motion capture test artefact and the exoskeleton motion capture plate repeatability of the population was based on the test subject data. Plot (a) and (b) show the human and exoskeleton, respectively, knee joint angle measurement repeatability at the median, 95th, and 99th percentiles.

### 3.2 Evaluation of exoskeleton fit to user

To characterise the fit of the exoskeleton for the knee bend test in this study, the standard normal CDF (Figure 8) was derived from the offset between the exoskeleton articulation and the test subject’s knee joint angle (mean removed). The resulting estimated human-exoskeleton knee joint angle alignment used to establish the exoskeleton fit-to-user metric ranged between  $6.4^\circ$  to  $18.8^\circ$  (50th to 99th percentile). Note the maximum misalignment was when an equipment malfunction occurred. While the data should be discarded when evaluating an exoskeleton with respect to a specific task, the data was applied with the objective of capturing the exoskeleton fit to user in this study under nominal and anomalous circumstances.

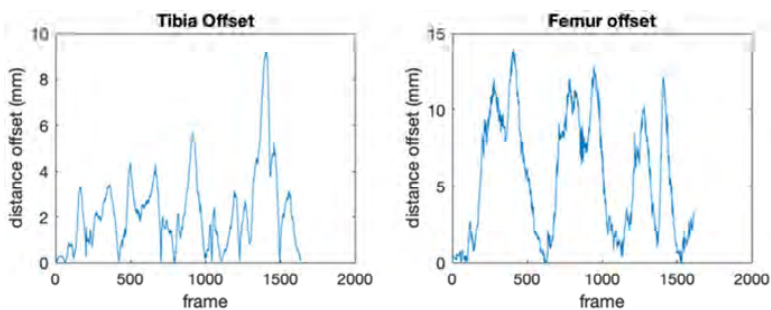
**Figure 8** Evaluation of exoskeleton fit to test subjects based on the angle difference between the human motion capture test artefacts and the exoskeleton motion capture plates (see online version for colours)



Notes: As a metric for exoskeleton fit, the median angle difference between the human and exoskeleton motion plates based on the standard normal CDF derived from the experimental data, was  $6.4^\circ$ , and approximately  $15.1^\circ$  and  $18.8^\circ$ , at 95th and 99th percentiles, respectively.

While this study focused on the fit along the sagittal plane, the human and exoskeleton motion capture plates can also be used to evaluate the fit along the transverse and coronal planes. For the transverse plane, the variations in distance between the exoskeleton and human motion capture test artefacts' femur and tibia plates, mean removed, can be observed during the dynamic motions as shown in Figure 9.

**Figure 9** Variations on the order of 10 mm to 15 mm between the exoskeleton and human motion capture plates, mean removed, were observed during a dynamic knee bend trial, showing variations in attachment (see online version for colours)



### 3.3 Test subject stability

An important safety consideration for the exoskeleton user is stability. Ideally, the human-exoskeleton interface enables a balanced posture. A stability metric, the balance angle, was computed as the angle between the instantaneous normal vector and the average normal vector (normalised) of the exoskeleton plane as determined by the marker positions on the exoskeleton motion capture plates as shown in Figure 10.

**Figure 10** Subject stability analysis process

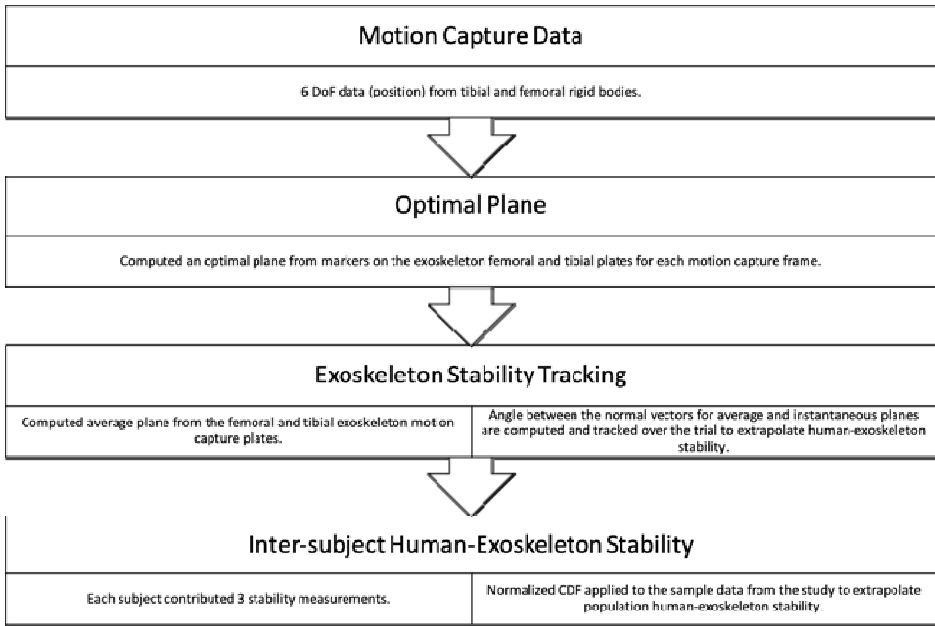
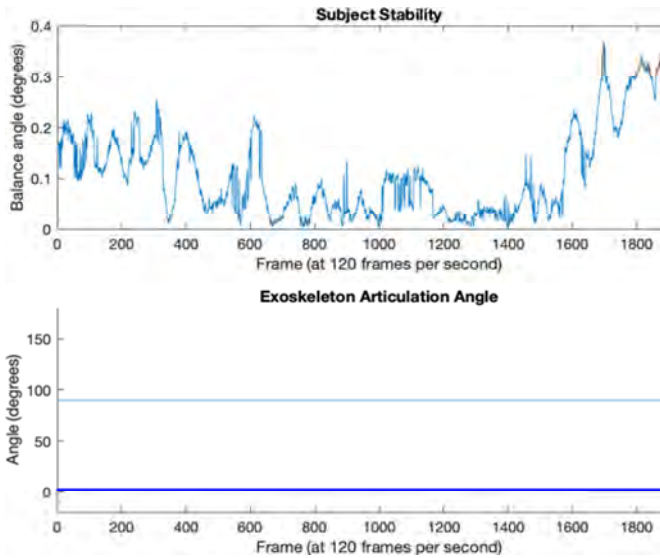


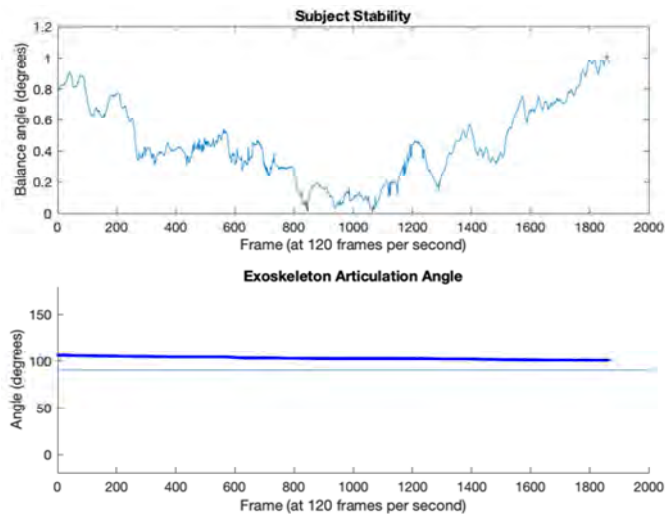
Figure 11 shows the variation in the angle between the instantaneous normal vector and the average normal vector during a standing, squatting, and dynamic knee bend trial. The balance angle variation was below  $0.4^\circ$  during the standing trial and increased during the static squatting and dynamic knee bend trials. For the dynamic knee bend trial, the instability peaks in the upper graph appeared to align with the extension phase of the knee bend cycle, potentially indicating the applied torque setting may have destabilised the test subject during the extension phase. However, the largest contributor of the balance angle may be due to the test subject’s motions, causing the exoskeleton’s plane to deviate from being perpendicular to the floor.

In this analysis, a CDF of the standard normal distribution extrapolated from an empirical CDF was applied. The range of human-exoskeleton stability from this study is shown in Figure 12. The variation between the average normal and the instantaneous normal was  $4.4^\circ$  at the 50th percentile and  $8.4^\circ$  at the 99th percentile.

**Figure 11** Dynamic stability of the test subject, based on the angle between the instantaneous normal and the average normal of the exoskeleton plane using the proximal and distal segments of the exoskeleton motion capture plates, (a) subject stability during a standing trial (b) subject stability during a squatting trial (c) subject stability within a single dynamic knee bend trial (see online version for colours)



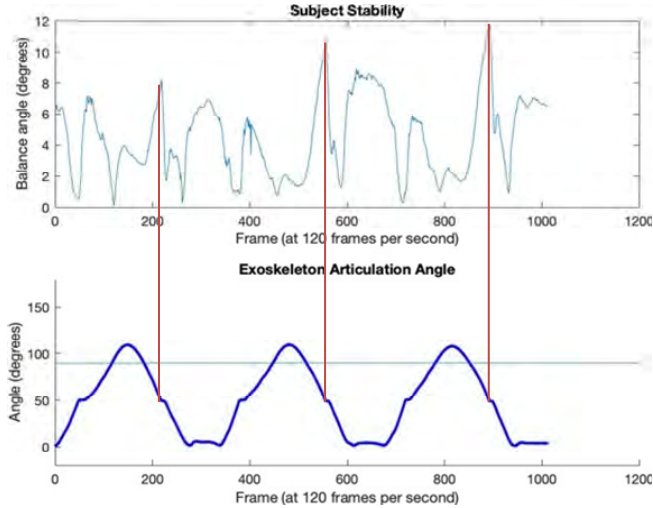
(a)



(b)

Notes: Bottom graphs track the exoskeleton kinematics based on the joint articulation angle. The instability peaks in the upper graph appeared to align with the extension phase of the knee bend cycle.

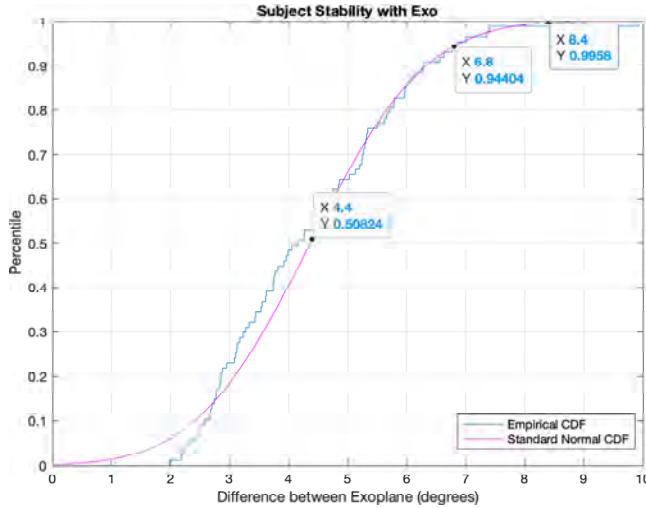
**Figure 11** Dynamic stability of the test subject, based on the angle between the instantaneous normal and the average normal of the exoskeleton plane using the proximal and distal segments of the exoskeleton motion capture plates, (a) subject stability during a standing trial (b) subject stability during a squatting trial (c) subject stability within a single dynamic knee bend trial (continued) (see online version for colours)



(c)

Notes: Bottom graphs track the exoskeleton kinematics based on the joint articulation angle. The instability peaks in the upper graph appeared to align with the extension phase of the knee bend cycle.

**Figure 12** Evaluation of subject stability based on the angle difference between the average and instantaneous normal of the exoskeleton plane derived from the exoskeleton motion capture plates (see online version for colours)



Note: As a metric for stability, the standard normal CDF, based on the angle difference computed from the experimental data, was approximately 4.4°, 6.8°, and 8.4°, at the 50th, 95th, and 99th percentiles, respectively.

## 4 Discussion

This study describes and evaluates a set of human motion capture test artefacts and exoskeleton motion capture test plates that simultaneously and independently track the knee joint angle of the lower-extremity exoskeleton and the test subject's knee with intra-subject repeatability within  $3^\circ$ , which is comparable to the current motion capture methods based on the literature review. The study further demonstrated how the human motion capture artefacts and exoskeleton motion capture plates can be applied to derive metrics for evaluating the *exoskeleton fit-to-user* and the *human-exoskeleton system stability*.

### 4.1 Motivation for the motion capture test artefacts and plates

The benefits of the human motion capture test artefacts and the exoskeleton motion capture plates are:

- 1 ease of attachment to the exoskeleton
- 2 ease and adjustability to fit all test subjects while wearing typical industrial work attire
- 3 elimination of marker placement on the skin, which may be impractical while wearing an exoskeleton as the test subject's clothing serves as a protective layer against pressure and friction from exoskeleton components
- 4 reduction of marker occlusion from the exoskeleton
- 5 independent and simultaneous kinematic tracking of the exoskeleton knee articulation and human knee joint angle.

The human motion capture test artefacts are intended to lower the cost and reduce time to test and evaluate the performance of industrial lower-limb exoskeletons. When wearing industrial exoskeletons, it is useful to wear typical work attire for the safety and comfort of the user. The human motion capture test artefacts mitigate marker occlusions from an exoskeleton by including markers on the front, left and right sides of the leg segments. Furthermore, by surrounding the human motion capture test artefacts with markers, the rigid body model derived from the marker cluster was intended to estimate the underlying bone segments, comprising the femur and tibia. Validation of the biomechanical accuracy, the accuracy of the relative knee joint angle derived from the human motion capture test artefacts compared to the human skeletal knee joint angles, of the study's methods to estimate the knee joint angle was outside the scope of this study.

The use of human motion capture test artefacts and exoskeleton test plates are intended to facilitate the development of objective metrics to assess the exoskeleton fit-to-user. The development and evaluation of quantifiable measures, compared to subjective measures, for evaluating exoskeleton fit and comfort, remains a challenge when working with a potentially diverse subject pool. Subjective measures are often biased by a subject's prior experience, tolerance, and interpretation of the survey questions, and can be difficult to correlate with objective metrics. For example, one person's level of comfort and tolerance of the exoskeleton can be variable and can also depend on one's psychosocial state given a particular day. Therefore, the primary motivation of providing an objective metrics is to alleviate the subjective variability.

## 4.2 *Measurement repeatability*

The repeatability of the subject knee joint angle estimates derived from the pair of human motion test artefacts for the knee joint angle, ranged from  $1.2^{\circ}$  to  $2.7^{\circ}$  at the 50th and 99th percentiles, respectively. In this study, the human motion capture test artefacts reduced variability, within  $3^{\circ}$  at the 99th percentile, when compared to markers attached directly to the skin, which varied as much as  $6^{\circ}$  to  $24.3^{\circ}$  based on literature review (Brown and Stanhope, 1995; Akbarshahi et al., 2010). The results from this study were comparable to the joint angle measurement repeatability from previous use of marker clusters with anatomical calibrations, which ranged from  $1.8^{\circ}$  to  $2.9^{\circ}$  on average for inter-trial measurements with humans only (Charlton et al., 2004). The repeatability of the exoskeleton knee joint angle derived from the exoskeleton motion capture plates was  $1.2^{\circ}$ ,  $2.5^{\circ}$ , and  $3.1^{\circ}$ , at the 50th, 95th, and 99th percentiles, respectively. Therefore, the exoskeleton motion capture plates used in the study can meet the established criterion at the 95th percentile. In contrast to the evaluation of the human and exoskeleton motion capture plates on the knee test apparatus (Bostelman et al., 2020), this study included the human factor. The decrease in repeatability of the exoskeleton marker plates was likely due to the variability of the test subjects, the fit of the test artefacts, and marker ambiguities or occlusions. Each test subject's anthropometry, response to the human-exoskeleton interface, and physical fitness can contribute to additional variability.

## 4.3 *Human-exoskeleton knee kinematics*

Figure 6 illustrates how the human motion capture test artefacts can track the human knee motion and the exoskeleton motion capture plates can synchronously track the exoskeleton knee joint motion. The kinematic trajectories of the human knee and exoskeleton joints indicate how the test subject engages with the forces at the exoskeleton's knee joint. The trajectory also shows how in this instance, the first repetition requires the most time for the test subject to engage sufficient force to continue to a full squat. Additionally, the joint angle offset between the human knee and the exoskeleton knee appears to peak during the squat. This deviation needs to be further explored. It may be due to the alignment of the marker cluster relative to the femur and tibia bones which can deviate as much as  $15^{\circ}$  for the knee joint angle (Sangeux et al., 2006) or a misalignment during the maximum flexion phase. Further analysis and improvements may be needed to improve the modeling of the knee joint angle during the flexion phase.

## 4.4 *Exoskeleton fit-to-user*

For optimal human-exoskeleton dynamics, the exoskeleton should assist in synchrony with the user. Minimising joint angle difference between the exoskeleton and the test subject's knee would reduce interference to the user's movement. The kinematics analysis from tracking the human motion capture artefacts and the exoskeleton motion capture plates indicated that the separation in angle alignment begins in the flexion phase and peaks upon reaching maximum flexion, as shown in Figure 6. Additionally, lower limb exoskeletons are designed to support users in strenuous positions such as a squat. While the results from the synchronous human-exoskeleton knee joint angle estimates indicate variations in alignment over time, the largest misalignment often occurred during

the knee joint flexion phase. Therefore, the metric used to evaluate the exoskeleton fit-to-user was to simply compute the mean angle difference between the angle of the exoskeleton motion capture plates and the angle of the human motion capture test artefacts during the static, maximum flexion trial for each test subject.

There are several challenges with evaluating exoskeleton fit on individuals. Many factors can impact the fit of the exoskeleton. Such factors include, but are not limited to, the test subject anthropometry, which may or may not affect the fit of the user and the task being performed. Other factors impacting the exoskeleton fit-to-user included the task performed, the exoskeleton, and any knee joint angle estimation or OTS measurement error. The study was also limited to visual assessment of the alignment of the exoskeleton knee joint to the test subject's knee joint based on still photo and video capture. Additional correlation studies based on subjective fit and comfort input from the test subject would provide additional insights in evaluating or expanding on the exoskeleton fit-to-user. For example, having the test subject's perspective on the general comfort as well as areas of discomfort prior to, during, and after the task completion can provide an understanding of whether the cause of the discomfort is due to a fit configuration. The frequency of discomforts in a specific area can also be evaluated among different test subjects to address potential fit issues over a population. Experimentation with intentional misalignment on a variety of subjects and understanding the contribution of each uncertainty factor in the measurement of human-exoskeleton misalignment also requires further study. Additionally, metrics to capture the dynamic variations across the sagittal, transverse, and coronal planes in the exoskeleton fit are also needed to verify whether an exoskeleton can properly align to the user during a task. Tracking the position and orientation of the marker plates along the transverse and coronal plane during a trial can also provide insights on how well the exoskeleton was attached to the user. Alignment shifts along all three planes can potentially have adverse burdens on the test subjects, where an ideal human-exoskeleton knee joint alignment would have minimal variation in distance along the three planes.

#### 4.5 *Human-exoskeleton stability*

The test method along with the analysis algorithm s comprised one evaluation method to assess how an exoskeleton and the task can impact the stability of users. It was observed that some test subjects may not be accustomed to the assistive torque of an exoskeleton, and the additional weight and forces from an exoskeleton can destabilise a test subject. The sources of balance angle variations were due to a combination of the test subject's motion and the exoskeleton's attachment causing the exoskeleton plane to deviate from being perpendicular to the floor, human-exoskeleton instability, and measurement noise. The study assumed exoskeleton has a knee joint articulation constrained to the sagittal plane and that the task is limited to a test subject in a fixed location. Furthermore, the balance angle metric may have confounding sources of angle deviations, which included a combination of the test subject's motion and exoskeleton's attachment causing the exoskeleton plane to deviate from being perpendicular to the floor and measurement noise. Prior to using a stability metric based on kinematic data, a correlation study with kinetic measurements based on pressure sensors or force plates is needed.

Additionally, the test method is sensitive to variabilities in the test subject including their physical fitness and their psychosocial state. The psychosocial state of a test subject can impact their confidence and motivation, both of which can affect the human-

exoskeleton interactions, such as the overall system coordination and stability. The test subject confidence in the system can be their confidence in working with the exoskeleton or with the exoskeleton itself. Furthermore, when evaluating the human-exoskeleton stability for a specific exoskeleton, sample test subject demographic, and task, the torque at the exoskeleton knee joint should be adjusted to the preference of the test subject. The results are specific to this study's test protocol. Therefore, additional considerations are needed when applying and interpreting the human-exoskeleton stability metric for a specific exoskeleton, task, and user.

#### 4.6 Limitations of the study

The evaluation of the measurement method for motion capture test artefact repeatability in human subjects, human-exoskeleton system stability, and exoskeleton fit to test subject were limited by *the intra-subject and inter-subject variability*. The intra-subject variability can be due to the ability of the subject to repeat their motion exactly in each trial. As observed during the study, test subjects can become more accustomed to the exoskeleton or more fatigued, both of which can impact the test subject's range of motion or stability when executing a trial. Having only three repetitions was decided to reduce the physical strain and the time of each subject. The reserved time allowed the study to test more subjects to understand the motion capture test artefact repeatability across a broader range of subjects. The reduced number of trials is a limitation in understanding intra-subject repeatability. The inter-subject variability includes the physical fitness and coordination, which can impact stability, as well as the anthropometric differences that can impact the fit of an exoskeleton to a test subject. The results were also impacted by the human motion capture test artefact placement and movement during the task. Recent studies have shown that wearable sensors and marker clusters can also be sensitive to placement location, and that using a biomechanical model to optimise location of wearable sensors, potentially similar to human motion capture test artefacts, for an individual can improve the results (Derungs and Amft, 2020).

The study was also limited to the capture and analysis of *subject and exoskeleton knee kinematic data*. In addition to kinematics, the kinetics of lower-limb exoskeletons are also subject to variable dynamics due to human-exoskeleton interaction and potential transmission of pressures and forces (Zhang and Collins, 2017). Kinetic data will be needed to further evaluate the stability and fit metrics for accuracy and sensitivity while conducting specific industrial and mobility exoskeleton tests.

The analysis method was limited to estimating the *relative knee joint angles along the sagittal plane between the exoskeleton and the human motion capture test artefacts*. The calibration of the human motion capture artefacts to the human skeletal frame as well as the biomechanical accuracy of the measurements would require further study prior to standardisation. Future tests and analysis would expand on the study to

- 1 quantify the sensitivity of human knee joint angle estimate error and repeatability to size adjustments in the human motion capture test artefact using biomechanical simulation models and IMUs
- 2 assess the kinematic crosstalk and relative difference between the joint angle estimates of the human motion capture test artefacts against skeletal marker sets for biomechanics in all three planes, sagittal, transverse, and coronal planes

- 3 correlate the stability metric with human-exoskeleton kinetic measurement methods such as pressure mats, pressure insoles, or force plates
- 4 expand on the repeatability and reproducibility of the results using the human motion capture test artefacts by removing and replacing the test artefact on the same subject and with different exoskeletons
- 5 assess whether there are additional improvements in the human motion capture test artefact design and analytical methods to improve the measurement accuracy and repeatability.

The test method also collected *limited anthropometric and demographic data*. The study was not intended to test the exoskeleton performance itself, which may be more sensitive to demographic and anthropometric differences than the human motion capture test artefacts and exoskeleton motion capture plates. Testing the exoskeleton performance may require a familiarisation protocol depending on the complexity of the human-exoskeleton interface for the subject to effectively cooperate with the exoskeleton's capabilities. Also test subjects comprised of intended users with similar demographic characteristics, e.g., potential exoskeleton users from a manufacturing site, would provide the necessary insight on whether exoskeleton provided the necessary fit and stability to the intended population of users with similar characteristics.

Additional limitations of the study included the use of *a single passive exoskeleton model, the range of motion the task required, and the type of tasks*. For example, the subject was requested to perform three knee bends in a fixed location in the volume without explicit instructions on the depth and speed of each knee bend. While some industrial tasks are relatively stationary, others may be more mobile or within a larger area. For certain mobility tests that may cause structural or subject occlusions, such as navigating through a confined space and ascending or descending hurdles, the motion tracking quality may be degraded. To address such issues, the flexibility and ease of markerless pose estimation techniques are being developed (Vlasic et al., 2007; Gall et al., 2009; Cao et al., 2018), which can rely on kinematic and kinetic measurements to infer pose data despite occlusions. Once the repeatability and accuracy of the motion capture test artefacts have been fully characterised, future applications of using the human motion capture test artefacts and exoskeleton motion capture plates are to use marker-based techniques as a ground truth to evaluate the markerless pose estimation and other sensor-based methods that allow untethered, synchronous evaluation of human-exoskeleton kinematics.

The fit-to-user and human-exoskeleton stability metrics and results from the study are intended to illustrate how the 6DoF estimates from the human motion capture test artefacts and exoskeleton motion capture test plates can be used to assess human-exoskeleton interaction. Correlations studies with kinetic measurements and subjective comfort information are needed for a better understanding of how well the metrics capture exoskeleton fit-to-user in terms of providing balance and comfort to the exoskeleton user. Additional experimentation with different exoskeletons and tasks is needed to evaluate the adaptability and applicability of the motion capture test artefacts and plates for a broader range of human-exoskeleton interactions.

## 5 Conclusions

The main contribution of this study is the development and evaluation of a pair of human motion capture test artefacts and exoskeleton motion capture plates towards a standardised method for tracking exoskeleton and human kinematics to evaluate fit and other human-exoskeleton system performance metrics. This study evaluated the repeatability of estimating the relative joint angle between the rigid bodies of the motion capture test artefacts. The use of motion capture test artefacts offers a common and simple method for synchronously tracking the human-exoskeleton system dynamics by eliminating the need to place markers on anatomical landmarks and segments. Skeletal models may also need to be modified based on the exoskeleton frame and is often not readily transferable across different exoskeletons. The motion capture test artefacts allowed the test subjects to wear their typical work attire, reduced placement errors and occlusions by the exoskeleton, and strived to reduce movement errors. The human motion capture test artefact provided an adjustable, rigid structure to fit a range of subjects with comparable measurement repeatability to motion capture skeletal models. Synchronous tracking of human-exoskeleton knee kinematics can then be applied towards standardised metrics such as an exoskeleton's fit to user and human-exoskeleton stability for tasks in a fixed location.

## Disclaimer

Official contribution of the National Institute of Standards and Technology; not subject to copyright in the United States.

## References

- Akbarshahi, M., Schache, A.G., Fernandez, J.W., Baker, R., Banks, S. and Pandy, M.G. (2010) 'Non-invasive assessment of soft-tissue artifact and its effect on knee joint kinematics during functional activity', *Journal of Biomechanics*, Vol. 43, No. 7, pp.1292–1301.
- Alvarez, M., Torricelli, D., del Ama, A.J., Pinto, D., Gonzalez-Vargas, J., Moreno, J.C., Gil-Agudo, A. and Pons, J.L. (2017) 'Simultaneous estimation of human and exoskeleton motion: a simplified protocol', in *2017 International Conference on Rehabilitation Robotics (ICORR)*, IEEE, pp.1431–1436.
- Barbareschi, G., Richards, R., Thornton, M., Carlson, T. and Holloway, C. (2015) 'Statically vs. dynamically balanced gait: Analysis of a robotic exoskeleton compared with a human', in *2015 37th Annual International Conference of the IEEE Engineering in Medicine and Biology Society (EMBC)*, IEEE, pp.6728–6731.
- Biasi, N., Setti, F., Del Bue, A., Tavernini, M., Lunardelli, M., Fornaser, A., Da Lio, M. and De Cecco, M. (2015) 'Garment-based motion capture (gamocap): high-density capture of human shape in motion', *Machine Vision and Applications*, Vol. 26, Nos. 7–8, pp.955–973.
- Bostelman, R., Li-Baboud, Y-S., Van Wyk, K. and Shah, M. (2020) *Development of a Kinematic Measurement Method for Knee Exoskeleton Fit to a User*.
- Brown, M. and Stanhope, S. (1995) 'Preventing implementation and tracking errors from becoming clinical judgement errors in functional movement analysis', *Gait & Posture*, Vol. 3, No. 2, p.88.
- Cao, Z., Hidalgo, G., Simon, T., Wei, S-E. and Sheikh, Y. (2018) *Openpose: Realtime Multi-Person 2d Pose Estimation using Part Affinity Fields*, arXiv preprint arXiv:1812.08008.

- Cappozzo, A., Della Croce, U., Leading, A. and Chiari, L. (2005) 'Human movement analysis using stereophotogrammetry: Part 1: theoretical background', *Gait & Posture*, Vol. 21, No. 2, pp.186–196.
- Charlton, I., Tate, P., Smyth, P. and Roren, L. (2004) 'Repeatability of an optimised lower body model', *Gait & Posture*, Vol. 20, No. 2, pp.213–221.
- Chiari, L., Della Croce, U., Leardini, A. and Cappozzo, A. (2005) 'Human movement analysis using stereophotogrammetry: Part 2: Instrumental errors', *Gait & Posture*, Vol. 21, No. 2, pp.197–211.
- Choi, B., Lee, Y., Kim, J., Lee, M., Lee, J., Roh, S-G., Choi, H., Kim, Y-J. and Choi, J-Y. (2016) 'A self-aligning knee joint for walking assistance devices', in *2016 38th Annual International Conference of the IEEE Engineering in Medicine and Biology Society (EMBC)*, IEEE, pp.2222–2227.
- Cloete, T. and Scheffer, C. (2008) 'Benchmarking of a full-body inertial motion capture system for clinical gait analysis', in *2008 30th Annual International Conference of the IEEE Engineering in Medicine and Biology Society*, IEEE, pp.4579–4582.
- Collins, T.D., Ghousayni, S.N., Ewins, D.J. and Kent, J.A. (2009) 'A six degrees-of-freedom marker set for gait analysis: repeatability and comparison with a modified Helen Hayes set', *Gait & Posture*, Vol. 30, No. 2, pp.173–180.
- Derungs, A. and Amft, O. (2020) 'Estimating wearable motion sensor performance from personal biomechanical models and sensor data synthesis', *Scientific Reports*, Vol. 10, No. 1, pp.1–13.
- Diebel, J. (2006) 'Representing attitude: Euler angles, unit quaternions, and rotation vectors', *Matrix*, Vol. 58, Nos. 15–16, pp.1–35.
- Dorociak, R. and Cuddeford, T. (1995) 'Determining 3-d system accuracy for the Vicon 370 system', *Gait & Posture*, Vol. 3, No. 2, p.88.
- Exoskeleton Market Size 2020*, Market Watch, March [online] <https://www.marketwatch.com/press-release/exoskeleton-market-size-2020-trends-industry-share-growth-drivers-business-opportunities-and-demand-forecast-to-2026-2020-3-20?mod=mwquote> news.
- Fritsch, F.N. and Carlson, R.E. (1980) 'Monotone piecewise cubic interpolation', *SIAM Journal on Numerical Analysis*, Vol. 17, No. 2, pp.238–246.
- Gall, J., Stoll, C., De Aguiar, E., Theobalt, C., Rosenhahn, B. and Seidel, H-P. (2009) 'Motion capture using joint skeleton tracking and surface estimation', in *2009 IEEE Conference on Computer Vision and Pattern Recognition*, IEEE, pp.1746–1753.
- Grood, E.S. and Suntay, W.J. (1983) *A Joint Coordinate System for the Clinical Description of Three-Dimensional Motions: Application to the Knee*.
- Kadaba, M.P., Ramakrishnan, H. and Wootten, M. (1990) 'Measurement of lower extremity kinematics during level walking', *Journal of Orthopaedic Research*, Vol. 8, No. 3, pp.383–392.
- Knaepen, K., Beyl, P., Duerinck, S., Hagman, F., Lefeber, D. and Meeusen, R. (2014) 'Human–robot interaction: Kinematics and muscle activity inside a powered compliant knee exoskeleton', *IEEE Transactions on Neural Systems and Rehabilitation Engineering*, Vol. 22, No. 6, pp.1128–1137.
- Lebleu, J., Gosseye, T., Detrembleur, C., Mahaudens, P., Cartiaux, O. and Penta, M. (2020) 'Lower limb kinematics using inertial sensors during locomotion: accuracy and reproducibility of joint angle calculations with different sensor-to-segment calibrations', *Sensors*, Vol. 20, No. 3, p.715.
- Lowe, B.D., Billotte, W.G. and Peterson, D.R. (2019) 'ASTM F48 formation and standards for industrial exoskeletons and exosuits', *IIEE Transactions on Occupational Ergonomics and Human Factors*, Vol. 7, Nos. 3–4, pp.230–236.
- Manal, K., McClay, I., Stanhope, S., Richards, J. and Galinat, B. (2000) 'Comparison of surface mounted markers and attachment methods in estimating tibial rotations during walking: an in vivo study', *Gait Posture*, Vol. 11, No. 1, pp.38–45 [online] <https://www.sciencedirect.com/science/article/pii/S0966636299000429>.

- Masouros, S., Bull, A. and Amis, A. (2010) 'Biomechanics of the knee joint', *Orthopaedics and Trauma*, Vol. 24, No. 2, pp.84–91.
- Matlab Documentation: Filloutliers (2017) [online] <https://www.mathworks.com/help/matlab/ref/filloutliers.html> (accessed 18 May 2020).
- McFadden, C., Daniels, K. and Strike, S. (2020) 'The sensitivity of joint kinematics and kinetics to marker placement during a change of direction task', *Journal of Biomechanics*, Vol. 101, p.109635.
- McNamara, N.P. (2020) *Using Decision Trees to Predict Intent to Use Passive Occupational Exoskeletons in Manufacturing Tasks*, PhD dissertation, Ohio University.
- Mooney, L.M. and Herr, H.M. (2016) 'Biomechanical walking mechanisms underlying the metabolic reduction caused by an autonomous exoskeleton', *Journal of Microengineering and Rehabilitation*, Vol. 13, No. 1, pp.1–12.
- Motive Documentation: Calibration (2017) [online] <https://v110.wiki.optitrack.com/index.php?title=Calibration> (accessed 18 May 2020).
- Moylan, S., Slotwinski, J., Cooke, A., Jurrrens, K. and Donmez, M.A. (2014) 'An additive manufacturing test artifact', *Journal of research of the National Institute of Standards and Technology*, Vol. 119, p.429.
- Önen, Ü., Botsahi, F.M., Kalyoncu, M., Tınkır, M., Yılmaz, N. and Şahin, Y. (2013) 'Design and actuator selection of a lower extremity exoskeleton', *IEEE/ASME Transactions on Mechatronics*, Vol. 19, No. 2, pp.623–632.
- Peters, A., Galna, B., Sangeux, M., Morris, M. and Baker, R. (2010) 'Quantification of soft tissue artifact in lower limb human motion analysis: a systematic review', *Gait & Posture*, Vol. 31, No. 1, pp.1–8.
- Pillai, M.V., Van Engelhoven, L. and Kazerooni, H. (2020) 'Evaluation of a lower leg support exoskeleton on floor and below hip height panel work', *Human Factors*, Vol. 62, No. 3, pp.489–500.
- Poitras, I., Dupuis, F., Biemann, M., Campeau-Lecours, A., Mercier, C., Bouyer, L.J. and Roy, J-S. (2019) 'Validity and reliability of wearable sensors for joint angle estimation: a systematic review', *Sensors*, Vol. 19, No. 7, p.1555.
- Sangeux, M., Marin, F., Charleux, F., Du`rselen, L. and Tho, M.H.B. (2006) 'Quantification of the 3d relative movement of external marker sets vs. bones based on magnetic resonance imaging', *Clinical Biomechanics*, Vol. 21, No. 9, pp.984–991.
- Schmidt, J., Berg, D.R., Ploeg, H-L. and Ploeg, L. (2009) 'Precision, repeatability and accuracy of Optotrak optical motion tracking systems', *International Journal of Experimental and Computational Biomechanics*, Vol. 1, No. 1, pp.114–127.
- Sposito, M., Di Natali, C., Toxiri, S., Caldwell, D.G., De Momi, E. and Ortiz, J. (2020) 'Exoskeleton kinematic design robustness: an assessment method to account for human variability', *Wearable Technologies*, Vol. 1.
- Talaty, M., Esquenazi, A. and Briceno, J.E. (2013) 'Differentiating ability in users of the Rewalk powered exoskeleton: an analysis of walking kinematics', in *2013 IEEE 13th International Conference on Rehabilitation Robotics (ICORR)*, IEEE, pp.1–5.
- Tang, S., Chen, L., Barsotti, M., Hu, L., Li, Y., Wu, X., Bai, L., Frisoli, A. and Hou, W. (2019) 'Kinematic synergy of multi-DOF movement in upper limb and its application for rehabilitation exoskeleton motion planning', *Frontiers in Neurobotics*, Vol. 13, p.99.
- Vlasic, D., Adelsberger, R., Vannucci, G., Barnwell, J., Gross, M., Matusik, W. and Popovic, J. (2007) 'Practical motion capture in everyday surroundings', *ACM Transactions on Graphics (TOG)*, Vol. 26, No. 3, pp.35–es.
- Wang, J., Li, X., Huang, T-H., Yu, S., Li, Y., Chen, T., Carriero, A., Oh-Park, M. and Su, H. (2018) 'Comfort-centered design of a lightweight and back drivable knee exoskeleton', *IEEE Robotics and Automation Letters*, Vol. 3, No. 4, pp.4265–4272.

- Zanotto, D., Akiyama, Y., Stegall, P. and Agrawal, S.K. (2015) 'Knee joint misalignment in exoskeletons for the lower extremities: effects on user's gait', *IEEE Transactions on Robotics*, Vol. 31, No. 4, pp.978–987.
- Zhang, J. and Collins, S.H. (2017) 'The passive series stiffness that optimizes torque tracking for a lower-limb exoskeleton in human walking', *Frontiers in Neurobotics*, Vol. 11, p.68.

## **Notes**

- 1 Certain commercial equipment, instruments, or materials are identified in this paper to foster understanding. Such identification does not imply recommendation or endorsement by the National Institute of Standards and Technology, nor does it imply that the materials or equipment identified are necessarily the best available for the purpose.